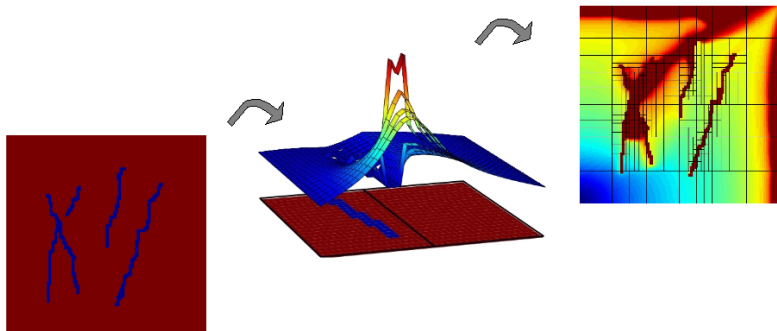


Multiscale Methods for Subsurface Flow

Jørg Aarnes, Knut-Andreas Lie, Stein Krogstad, and Vegard Kippe
SINTEF ICT, Dept. of Applied Mathematics



... and for saving our planet

Groundwater hydrological systems

“... the world faces a water crisis that, left unchecked, will derail the progress towards the Millennium Development Goals and hold back human development.”

UN's Human Development Report 2006

Modeling is needed to

- acquire general knowledge of groundwater basins,
- quantify limits of sustainable use, and
- monitor transport of pollutants in the subsurface.

Storage of greenhouse gases in underground repositories

“Scientific and economical challenges still exist, but none are serious enough to suggest that carbon capture and storage will not work at the scale required to offset trillions of tons of CO₂ emissions over the next century.”

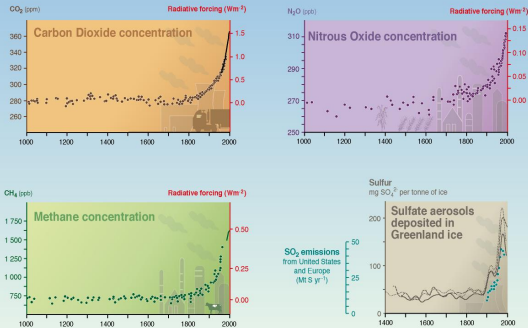
D. P. Schrag, Science, 2007

Modeling is needed to assess leakage rates (CO₂ must be stored long enough to allow the natural carbon cycle to reduce the atmospheric CO₂ to near pre-industrial level).

Indicators of human influence on the atmosphere

Source: www.ipcc.ch

Indicators of the human influence on the atmosphere during the Industrial era



SYR - FIGURE 2-1
WG1 FIGURE SPM-2

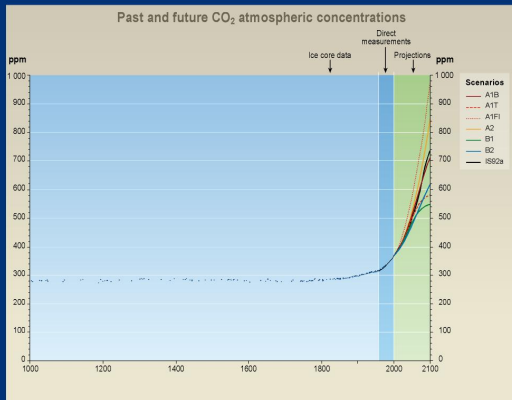
IPCC

INTERGOVERNMENTAL PANEL ON CLIMATE CHANGE



Past and future CO₂ atmospheric concentrations

Source: www.ipcc.ch



SYR - FIGURE 9-1a

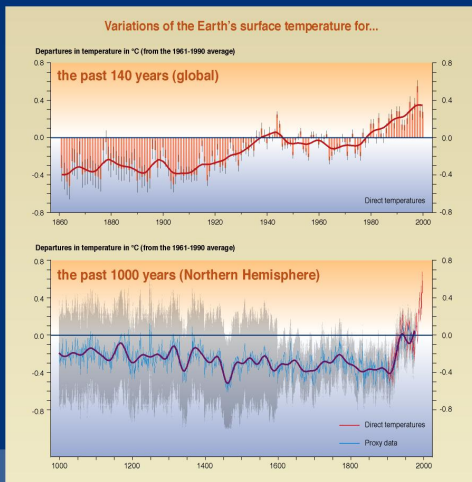
IPCC

INTERGOVERNMENTAL PANEL ON CLIMATE CHANGE



Variations of the Earth's surface temperature

Source: www.ipcc.ch



SYR - FIGURE 2-3

IPCC

INTERGOVERNMENTAL PANEL ON CLIMATE CHANGE



Reservoir modeling and simulation

The main purpose of reservoir simulation is to provide an information database to help position and manage wells and well trajectories in order to maximize the oil and gas recovery.

Despite more than 50 years of collaborative research efforts, reservoir simulation models are not sufficiently predictive due to ...

- incomplete geological description of the reservoir
- simulators cannot exploit all available information

Scales in subsurface flow

Subsurface flow is influenced by geological structures on a continuous spectrum of length scales.



Scales in subsurface flow

Subsurface flow is influenced by geological structures on a continuous spectrum of length scales.



Bad news:

All length scales have strong impact on flow patterns!

Scales in subsurface flow

Subsurface flow is influenced by geological structures on a continuous spectrum of length scales.



Bad news:

All length scales have strong impact on flow patterns!

Good news:

Modeling subsurface flow is a Mecca for multiscale methods.

It is impossible to resolve all scales in numerical models.

Upscaling and old multiscale approaches

Compute parameters that give correct averaged flow response.

- Homogenization – asymptotic analysis for periodic structures.
- Flow-based upscaling – solving local problems numerically to derive effective parameters for coarse scale simulation.
- Wavelet, multi-resolution, renormalization, etc.

Lack of robustness: Fine scale properties are not incorporated into the coarse scale model in a way that is consistent with the local property of the governing differential equations.

Novel multiscale methods for subsurface flow:

Build special finite-element approximation spaces that incorporate the impact of subgrid heterogeneity.

- Utilizing more geological data.
- Provide more accurate solutions.
- Have more geometric flexibility.

Status:

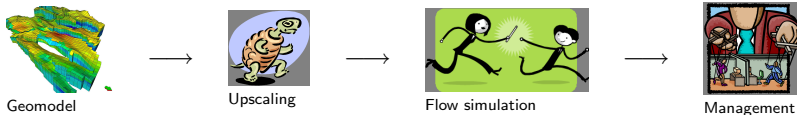
Multiscale methods are currently being implemented in (at least) two of the most commonly used reservoir simulators.

Today:

Geomodels too large and complex for flow simulation:
Upscaling performed to obtain

- Simulation grid(s).
- Effective parameters and pseudofunctions.

Simulation workflow



Tomorrow:

Earth Model shared between geologists and engineers —
Simulators take Earth Model as input.

- 1 Crash course on reservoir simulation (– 9.40)
 - Reservoir description
 - Reservoir simulation model
 - Production processes
- 2 Discretizing the pressure equation (9.40 – 10.20)
 - Basic discretization techniques for the pressure equation
 - Upscaling permeability for the pressure equation
- 3 Multiscale methods for the pressure equation (10.30 – 11.20)
 - Multiscale finite-element method (MsFEM)
 - Multiscale finite-volume method (MsFVM)
 - Multiscale mixed finite-element method (MsMFEM)
- 4 Implementational issues for the MsMFEM (11.30 – 12.00)
 - Generation of coarse grids
 - Computation of basis functions and assembly of linear system
 - Special issues

The reservoir

Subsurface formation containing compressed organic material that has evolved into hydrocarbon components, and prevented from migrating to the surface by non-permeable rock.

Geological model: the geologist's conception of the reservoir

A geostatistical model providing a plausible characterization of the geometry, porosity, and permeability of the reservoir.

Simulation model: a framework for predicting flow responses

A (coarsened) geological model supplied with a system of partial differential equations, and a corresponding set of flow parameters.

Porosity ϕ : fraction of void volume in the rock subject to flow.

The *porosity* is usually assumed to depend linearly on pressure p :

$$\phi = \phi_0(1 + c_r(p - p_0)),$$

where p_0 is a specified reference pressure and $\phi_0 = \phi(p_0)$.

Permeability K : measure of the rock's ability to transmit flow.

Permeability is measured in Darcy (D) ($1 \text{ D} \approx 0.987 \cdot 10^{-12} \text{ m}^2$).

Typical permeability values in an oil reservoir are 1 mD – 10 D.

The *permeability* is normally strongly correlated to ϕ , but, due to varying orientation and interconnection of the pores: K depends on direction, i.e., K is a symmetric and positive definite tensor.

The simulation model

The mathematical model for subsurface flow is derived solely from

- Darcy's law (after the french engineer Henri Darcy).
- Mass balance of each hydrocarbon component.

Darcy's law

Flow in porous media is driven by pressure p and gravity forces:

$$v \sim -K(\nabla p + \rho g \nabla z).$$

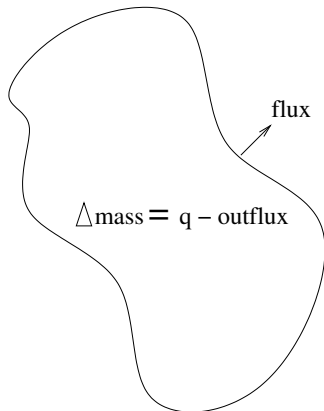
ρ = density, g = gravitational acceleration, z = vertical coordinate.

Mass balance

For each hydrocarbon component we require

$$\frac{\partial}{\partial t} (\phi \rho s) + \nabla \cdot (\rho v) = q.$$

s = fraction of void occupied by the hydrocarbon component.



Forcing mass balance over a volume V :

$$\begin{aligned}\Delta \text{mass} &= \int_V \phi \Delta(\rho s) dx \\ &= \int_V q - \nabla \cdot (\rho v) dx \\ &= \int_V q dx - \int_{\partial V} \rho v \cdot n ds \\ &= \text{accumulated source} - \text{outflux.}\end{aligned}$$

(n = outward unit normal on ∂V .)

Darcy's law for single-phase flow

Darcy's law is an empirical law modeling the volumetric flow density v (henceforth called flow velocity):

$$v = -\frac{K}{\mu}(\nabla p + \rho g \nabla z).$$

Darcy's law is analogous to Fourier's law (K = heat conductivity) and Ohm's law (K = inverse of the electrical resistance).

However, whereas there is only one driving force in thermal and electrical conduction, there are two driving forces in Darcy's law.

Example:

$$K = \begin{bmatrix} k_{xx} & k_{xy} & k_{xz} \\ k_{yx} & k_{yy} & k_{yz} \\ k_{zx} & k_{zy} & k_{zz} \end{bmatrix} \quad \nabla p = \begin{bmatrix} 1 \\ 0 \\ 0 \end{bmatrix} \quad \Rightarrow \quad v = -\frac{1}{\mu} \begin{bmatrix} k_{xx} \\ k_{yx} \\ k_{zx} + \rho g \end{bmatrix}$$

Grouping of hydrocarbon components

Since the number of hydrocarbon components (methane, ethane, propane, etc.) can be quite large, one groups different components together and only distinguish between water, oil, and gas.

Separating components into phases

Darcy's law describes the flow of phases, i.e., a mixture of components that have similar flow properties. Standard simulation models consider three separate phases, aqueous, liquid, and vapor.

- The aqueous phase does not mix with liquid and vapor.
- The liquid phase contains oil and liquidized gas.
- The vapor phase contains gas and vaporized oil.

Pressure: p_i (phase pressures differ due to surface tension).

Saturation s_i : volume fraction of void occupied by phase i .

$$\sum_i s_i = 1.$$

Mass fraction $m_{\alpha,i}$: fraction of component α in phase i .

$$\sum_{\alpha} m_{\alpha,i} = 1.$$

Density: $\rho_i = \rho_i(p_i, \{m_{\alpha,i}\})$.

Viscosity: $\mu_i = \mu_i(p_i, \{m_{\alpha,i}\})$

Capillary pressure: $p_{cij} = p_i - p_j$.

Compressibility: $c_i = (d\rho_i/dp_i)/\rho_i$.

Relative permeability:

The permeability experienced by one phase is reduced by the presence of other phases. The *relative permeability* functions

$$k_{ri} = k_{ri}(s_a, s_v), \quad \sum_i k_{ri} < 1,$$

are nonlinear functions that attempt to account for this effect.

Darcy's law for multi-phase flow:

The effective permeability experienced by phase i is then $K_i = Kk_{ri}$. Consequently, Darcy's law for phase i reads

$$v_i = -\frac{Kk_{ri}}{\mu_i} (\nabla p_i + \rho_i g \nabla z).$$

For multi-phase flow we require mass balance of each component:

$$\sum_i \frac{\partial}{\partial t} (\phi m_{\alpha,i} \rho_i s_i) + \sum_i \nabla \cdot (m_{\alpha,i} \rho_i v_i) = q_{\alpha},$$

Thus, we accumulate the mass of component α in each phase.

Pressure equation

The system of mass balance equations may be written on the form

$$\frac{\partial}{\partial t} (\phi A [s_i]) + \nabla \cdot (A [v_i]) = [q_{\alpha}], \quad i = a, l, v, \quad \alpha = w, o, g.$$

Multiplying with A^{-1} and summing the eqs. gives the *pressure eq*:

$$\frac{\partial \phi}{\partial t} + \phi [s_i] \cdot \left(A^{-1} \frac{\partial A}{\partial t} \right) \mathbf{1} + \sum_i \nabla \cdot v_i + [v_i] \cdot (A^{-1} \nabla A) \mathbf{1} = \mathbf{1} A^{-1} [q_{\alpha}].$$

Primary production: puncturing the balloon

When the first well is drilled and opened for production, trapped hydrocarbons start flowing (toward the well) due to over-pressure.

Secondary production: maintaining reservoir flow

As pressure drops, less oil and gas is flowing. To maintain pressure and push out more profitable hydrocarbons one starts injecting water or gas (or CO₂ in liquid form) into the reservoir.

Enhanced oil recovery (EOR): altering reservoir flow

EOR is used to alter flow patterns and fluid properties. E.g.,:

- Inject foam to more efficiently push out oil.
- Inject polymers to change the flow properties of water.
- Inject solvents to, e.g., develop miscibility with gas.

Three-phase three-component flow (black-oil model)

$$v_i = -\frac{Kk_{ri}}{\mu_i} (\nabla p_i + \rho_i g \nabla z),$$

$$\frac{\partial \phi}{\partial p_l} + \phi \sum_i c_i s_i \frac{\partial p_l}{\partial t} + \nabla \cdot \left(\sum_i v_i \right) + \sum_i c_i v_i \cdot \nabla p_l = q,$$

where the c_j s are phase compressibilities, and $q = \mathbf{1}A^{-1}[q_\alpha]$.

Incompressible flow with constant capillary pressure

$$v = -\lambda(\nabla p_l + \omega g \nabla z), \quad \nabla \cdot v = q.$$

where $v = \sum_i v_i$, $\lambda_i = Kk_{ri}/\mu_i$, $\lambda = \sum_i \lambda_i$, and $\omega = \sum_i \lambda_i \rho_i / \lambda$.

Mass conservation on a grid $\mathcal{G} = \{\Omega_i\}$

A method is (mass) conservative if

$$\int_{\Omega_i} \nabla \cdot v \, dx = \int_{\partial\Omega_i} v \cdot n \, ds = \int_{\Omega_i} q \, dx.$$

for each grid cell Ω_i in Ω (the reservoir).

Mass conservative methods

- Finite-volume methods
- Mixed finite-element methods
- Mimetic finite-difference methods

Finite volume methods have the following characteristics:

- Each equation imposes mass conservation for one grid cell:

$$\int_{\partial\Omega_i} v \cdot n \, ds = \int_{\Omega_i} q \, dx.$$

- Pressure is cell-wise constant.
- The outflux

$$\int_{\partial\Omega_i} v \cdot n \, ds$$

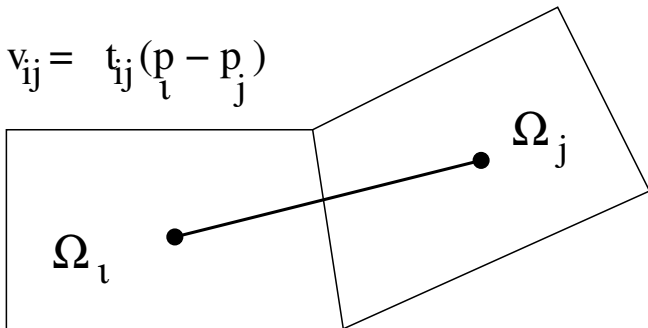
is estimated using Darcy's law with the pressure gradient defined in terms of neighboring pressure values.

The two-point flux-approximation (TPFA) scheme

TPFA:

Flux across $\gamma_{ij} = \partial\Omega_i \cap \partial\Omega_j$ is expressed as a function of p_i and p_j , the cell pressures in Ω_i and Ω_j , respectively.

$$v_{ij} = t_{ij}(p_i - p_j)$$



The two-point flux-approximation (TPFA) scheme

Discretized equations

Write the pressure equation (for incompressible flow) as follows:

$$-\nabla \cdot \lambda \nabla p = f,$$

where $f = q + g \partial_z(\lambda \omega)$. Then

$$\begin{aligned} f_i = \int_{\Omega_i} f \, dx &= - \int_{\partial\Omega_i} \lambda \nabla p \cdot n \, ds \\ &= - \sum_j \int_{\partial\Omega_i \cap \partial\Omega_j} \lambda \nabla p \cdot n_{ij} \, ds \\ &= \sum_j v_{ij} \approx \sum_j t_{ij} (p_i - p_j). \end{aligned}$$

Here n is the unit normal on $\partial\Omega_i$ pointing into Ω_j and n_{ij} is the unit normal on $\partial\Omega_i \cap \partial\Omega_j$ pointing into Ω_j .

The two-point flux-approximation (TPFA) scheme

Derivation of transmissibilities

On $\gamma_{ij} = \partial\Omega_i \cap \partial\Omega_j$ the TPFA scheme estimates

$$\nabla p \approx \partial p_{ij} = \left(\frac{p_j - p_i}{\text{dist}(c_i, c_j)} \right) n_{ij},$$

and assumes that on each interface $\lambda = \lambda_{ij}$ where λ_{ij} is a distance-weighted harmonic average of

$$\lambda_{i,ij} = n_{ij} \cdot \lambda_i n_{ij} \quad \text{and} \quad \lambda_{j,ij} = n_{ij} \cdot \lambda_j n_{ij}.$$

E.g., for an interface between two cells in the x -coordinate direction in a Cartesian grid with cell dimensions $(\Delta x_i, \Delta y_i, \Delta z_i)$:

$$\lambda_{ij} = (\Delta x_i + \Delta x_j) \left(\frac{\Delta x_i}{\lambda_{i,ij}} + \frac{\Delta x_j}{\lambda_{j,ij}} \right)^{-1}.$$

The two-point flux-approximation (TPFA) scheme

Derivation of transmissibilities, cont.

Thus,

$$v_{ij} = \int_{\partial\Omega_i \cap \partial\Omega_j} \lambda \nabla p \cdot n_{ij} ds \approx -|\gamma_{ij}| \lambda_{ij} \partial p_{ij} = t_{ij}(p_i - p_j),$$

where

$$t_{ij} = 2|\gamma_{ij}| \left(\frac{\Delta x_i}{\lambda_{i,ij}} + \frac{\Delta x_j}{\lambda_{j,ij}} \right)^{-1}.$$

The TPFA scheme results in a linear system of the form

$$\mathbf{A}\mathbf{p} = \mathbf{f} \quad \text{where} \quad a_{ik} = \begin{cases} \sum_j t_{ij} & \text{if } k = i, \\ -t_{ik} & \text{if } k \neq i. \end{cases}$$

Main limitation:

Example: Assume that K is a constant tensor and let γ_{ij} be an interface between two adjacent grid cells Ω_i and Ω_j in the x -coordinate direction in a Cartesian grid. Then

$$v_{ij} = - \int_{\gamma_{ij}} (k_{xx}p_x + k_{xy}p_y + k_{xz}p_z) ds.$$

Since p_i and p_j can not be used to estimate p_y and p_z , we see that the TPFA scheme neglects the contribution from $k_{xy}p_y$ and $k_{xz}p_z$.

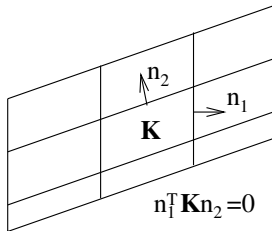
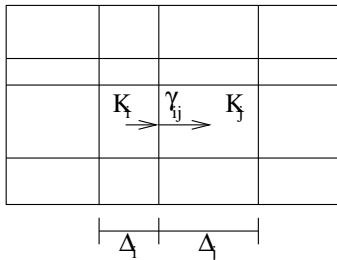
The two-point flux-approximation (TPFA) scheme

K -orthogonality

The TPFA scheme only convergent for K -orthogonal grids, i.e., grids where each cell is a parallelepiped and

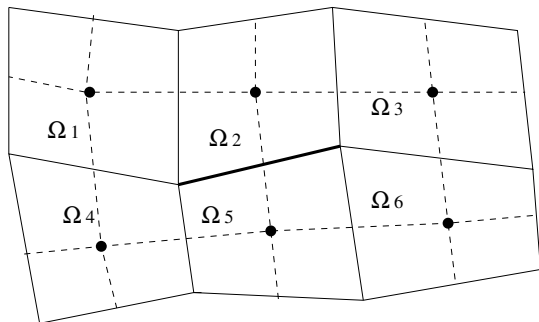
$$n_{ij} \cdot K n_{ik} = 0, \quad \forall \Omega_i \subset \Omega, \quad n_{ij} \neq \pm n_{ik}.$$

Examples:



Multi-point flux-approximation (MPFA) schemes

To obtain consistent interface fluxes for grids that are not K -orthogonal, one must also estimate partial derivatives in coordinate directions parallel to the interfaces.



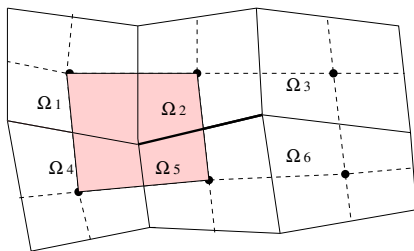
Solid line
= primal grid.

Dashed line
= dual grid.

To compute the flux across γ_{25} one uses cell pressures in cells 1–6.

Multi-point flux-approximation (MPFA) schemes

To derive an MPFA scheme it is common to introduce a dual grid.



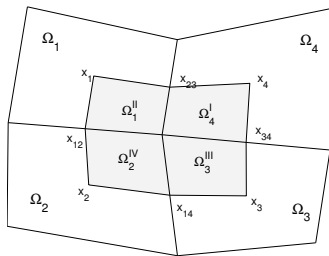
Example: Control-volume finite element method

Let V be the bilinear (trilinear) finite element space with respect to the dual grid, i.e., V is spanned by bilinear (trilinear) nodal basis functions where the nodes are cell centers in the primal grid.

$$\text{Find } p \in V \text{ such that } - \int_{\Omega_i} \lambda \nabla p \cdot n \, ds = \int_{\Omega_i} f \, dx.$$

Multi-point flux-approximation (MPFA) schemes

The O-method



O-method interaction region:

Region confined by edges or faces connecting the cell centers.

The shaded region is the interaction region associated with Ω_1 – Ω_4 .

Function space V for the O-method (quadrilateral grid):

- Each $v \in V$ is linear on each quadrant of \mathbb{R}^2 , and continuous at junction between the dual and primal grid.
- The flux normal to the interfaces of the primal grid $-\lambda \nabla v \cdot n_{ij}$ is continuous at junction between the dual and primal grid.

Pressure equation (incompressible flow):

$$v = -\lambda(\nabla p + \omega g \nabla z), \quad \nabla \cdot v = q.$$

Mixed formulation (no-flow boundary conditions):

Find $(p, v) \in L^2(\Omega) \times H_0^{\text{div}}(\Omega)$ such that

$$\begin{aligned} \int_{\Omega} v \cdot \lambda^{-1} u \, dx - \int_{\Omega} p \nabla \cdot u \, dx &= - \int_{\Omega} \omega g \nabla z \cdot u \, dx, \\ \int_{\Omega} l \nabla \cdot v \, dx &= \int_{\Omega} ql \, dx, \end{aligned}$$

for all $u \in H_0^{\text{div}}(\Omega)$ and $l \in L^2(\Omega)$.

Mixed finite-element method

Raviart-Thomas mixed finite-element method

In the Raviart–Thomas mixed FEM of lowest order (for triangular, tetrahedral, or regular parallelepiped grids), $L^2(\Omega)$ is replaced by

$$U = \{p = \sum_i p_i \chi_i\}, \quad \chi_i(x) = \begin{cases} 1 & \text{if } x \in \Omega_i, \\ 0 & \text{otherwise.} \end{cases}$$

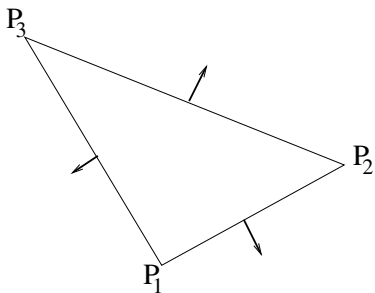
and $H_0^{\text{div}}(\Omega)$ is replaced by

$$V = \{v \in H_0^{\text{div}}(\Omega) \text{ such that} \\ v|_{\Omega_i} \text{ have linear components } \forall \Omega_i \in \Omega, \\ (v \cdot n_{ij})|_{\gamma_{ij}} \text{ is constant } \forall \gamma_{ij} \in \Omega, \\ \text{and } v \cdot n_{ij} \text{ is continuous across } \gamma_{ij}\}.$$

Mixed finite-element method

Raviart-Thomas mixed finite-element method for triangular grids

Restricted to a single triangle with corner-points P_1 , P_2 , P_3 in a triangular grid, the Raviart-Thomas mixed FEM space V is spanned by basis functions ψ_1 , ψ_2 , and ψ_3 .



$$\psi_1 = \alpha_1 \begin{pmatrix} x \\ y \end{pmatrix} - P_1,$$

$$\psi_2 = \alpha_2 \begin{pmatrix} x \\ y \end{pmatrix} - P_2,$$

$$\psi_3 = \alpha_3 \begin{pmatrix} x \\ y \end{pmatrix} - P_3.$$

$$\psi_1|_{E_{23}} \cdot n_{E_{23}} = \alpha_1 (P_2 + s(P_3 - P_2) - P_1) \cdot n_{E_{23}} = \alpha_1 (P_2 - P_1) \cdot n_{E_{23}}.$$

Mixed finite-element method

Raviart-Thomas mixed finite-element method

Find $p = \sum p_i \chi_i$ and $v = \sum_i \psi_i$ such that

$$\int_{\Omega} v \cdot \lambda^{-1} \psi_j \, dx - \int_{\Omega} p \nabla \cdot \psi_j \, dx = - \int_{\Omega} \omega g \nabla z \cdot \psi_j \, dx, \quad \forall j,$$
$$\int_{\Omega_j} \nabla \cdot v \, dx = \int_{\Omega_j} q \, dx, \quad \forall j.$$

Evaluation of integrals:

For the Raviart-Thomas mixed FEM, $\nabla \cdot \psi_j$ is cell-wise constant. Numerical integration is therefore employed only to evaluate

$$\int_{\Omega} v \cdot \lambda^{-1} \psi_j \, dx \quad \text{and} \quad \int_{\Omega} \omega g \nabla z \cdot \psi_j \, dx.$$

The integration is usually done using so-called Piola mappings to reference elements and numerical quadrature rules.

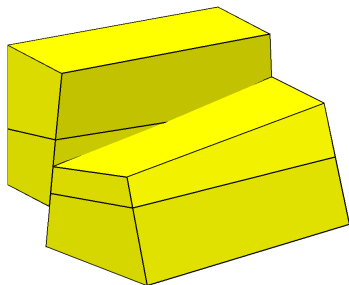
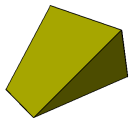
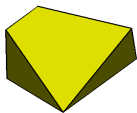
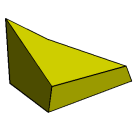
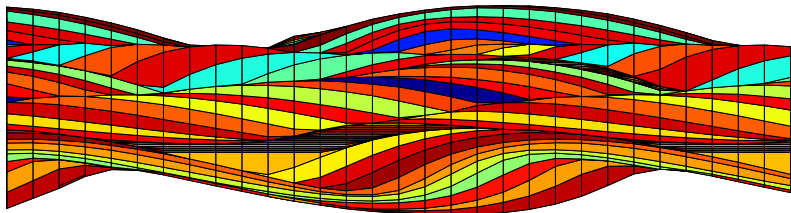
Are any of these methods satisfactory?

TPFA: Used by most commercial reservoir simulators, but are inaccurate because they are not designed for the type of grid models that are built today using modern geomodeling tools.

MPFA: More accurate than TPFA, but less robust and hard to implement for general grids, especially if the grid is non-conforming with non-matching faces.

MFEM: Accurate and quite robust, but cumbersome to implement – because different cells in geological models are generally not diffeomorphic, one needs a reference element and a corresponding Piola transform for each topological case.

Grid complexity issues to consider



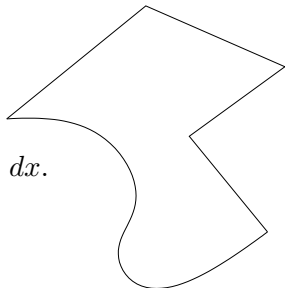
Mimetic FDMs:

Finite-difference-like mixed FEMs that avoid quadrature rules, reference elements, and Piola mappings: easy to implement, also for grids with irregular cell geometries and non-matching faces.

- Accuracy as low order MFEMs.
- Evaluates the integrals

$$\int_{\Omega} v \cdot \lambda^{-1} \psi_j \, dx \quad \text{and} \quad \int_{\Omega} \omega g \nabla z \cdot \psi_j \, dx.$$

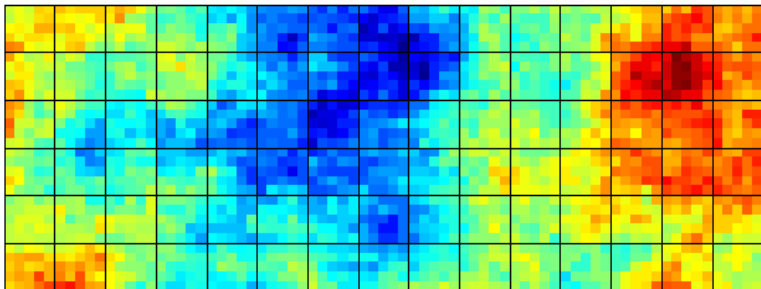
with an approximate bilinear form.



Why?

Geological parameters are given on a grid that is too fine for direct simulation with current simulators

— simple averaging generally gives inaccurate results.



Aim of upscaling procedures for the pressure equation:

Derive effective grid-block permeability tensors that produce the same flow response as the underlying geological grid-model.

Let p be the solution that we obtain by solving

$$-\nabla \cdot \lambda \nabla p = f, \quad \text{in } \Omega.$$

For each coarse grid-block V we seek a tensor λ_V^* such that

$$\int_V \lambda \nabla p \, dx = \lambda_V^* \int_V \nabla p \, dx.$$

I.e., the net flow-rate \bar{v} through V is related to the average pressure gradient $\overline{\nabla p}$ in V through Darcy's law $\bar{v} = -\lambda^* \overline{\nabla p}$.

Upscaling: Building a coarse grid model

The one-dimensional case

Consider the one dimensional pressure equation:

$$-\partial_x(\lambda p'(x)) = 0 \quad \text{in } (0, 1), \quad p(0) = p_0, \quad p(1) = p_1.$$

Here the Darcy velocity v is constant and $p'(x) \propto \lambda^{-1}$. Hence,

$$\int_0^1 p'(x) dx = p_1 - p_0 \quad \implies \quad p'(x) = \frac{p_1 - p_0}{\lambda} \left[\int_0^1 \frac{dx}{\lambda} \right]^{-1}.$$

Thus, for $(a, b) \subset (0, 1)$ we have

$$\int_a^b \lambda p'(x) dx = \left[\frac{1}{b-a} \int_a^b \frac{dx}{\lambda} \right]^{-1} \left[\frac{1}{b-a} \int_a^b p'(x) dx \right].$$

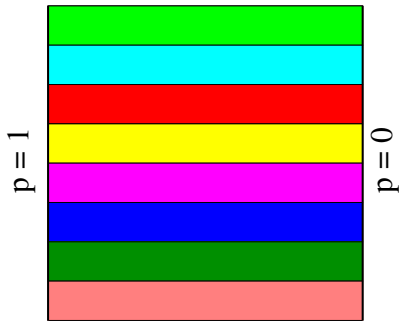
I.e., λ_V^* is identical to the harmonic mean for all $V \subset (0, 1)$.

Upscaling: Building a coarse grid model

Two special multi-dimensional cases

Flow from left to right

$$v \cdot n = 0$$

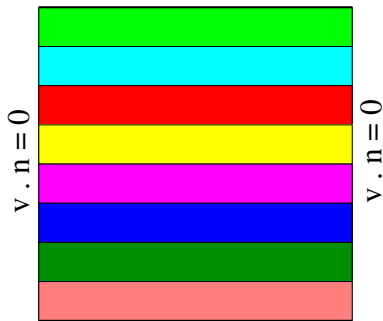


$$v \cdot n = 0$$

$\lambda^* = \text{arithmetic average}$

Flow from top to bottom

$$p = 1$$



$$p = 0$$

$\lambda^* = \text{harmonic average}$

Conclusion: correct upscaling depends on the flow.

Upscaling: Building a coarse grid model

Harmonic-arithmetic averaging

Harmonic-arithmetic averaging

To model flow in more than one direction, define a diagonal permeability tensor with the following diagonal components:

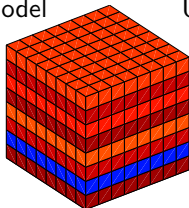
$$k_{xx} = \mu_a^z(\mu_a^y(\mu_h^x)), \quad k_{yy} = \mu_a^z(\mu_a^x(\mu_h^y)), \quad k_{zz} = \mu_a^x(\mu_a^y(\mu_h^z)).$$

Here μ_a^ξ and μ_h^ξ is the arithmetic and harmonic means in the ξ -coordinate direction.

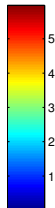
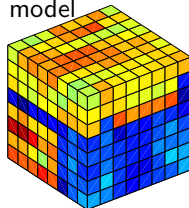
Harmonic-arithmetic averaging gives correct upscaling for perfectly stratified media with flow parallel to, or perpendicular to the layers.

Numerical example

Stratified model



Unstratified model



Boundary conditions:

BC1: $p = 1$ at $(x, y, 0)$, $p = 0$ at $(x, y, 1)$, else no-flow.

BC2: $p = 1$ at $(0, 0, 0)$, $p = 0$ at $(1, 1, 1)$, else no-flow.

Relative flow rate error	Stratified model		Unstratified model	
	BC1	BC2	BC1	BC2
Harmonic	1	5.52e-02	1.10e-02	9.94e-04
Arithmetic.	4.33e+03	2.39e+02	2.33e+04	2.13e+03
Harm. - Arit.	1	1.14	8.14e-02	1.55e-01

Flow based upscaling:

For each grid block V , solve the homogeneous equation

$$-\nabla \cdot \lambda \nabla p = 0 \quad \text{in } V,$$

with three sets of boundary conditions, one for each coordinate direction. Compute an upscaled tensor λ^* with components

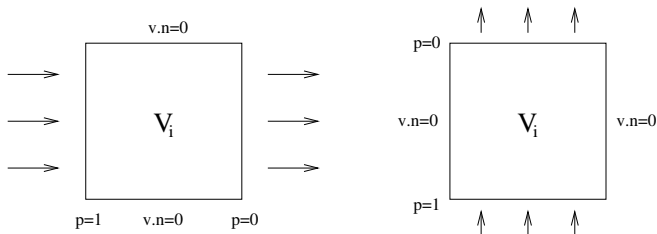
$$\lambda_{x\xi} = -Q_\xi L_\xi / \Delta P_x, \quad \lambda_{y\xi} = -Q_\xi L_\xi / \Delta P_y, \quad \lambda_{z\xi} = -Q_\xi L_\xi / \Delta P_z.$$

Here Q_ξ , L_ξ and ΔP_ξ are the net flow, the length between opposite sides, and the pressure drop in the ξ -direction.

Fundamental problem:

What kind of boundary conditions should be imposed?

Fixed boundary conditions (yields a diagonal tensor)



Periodic boundary conditions, x -direction

$$\begin{aligned} p(1, y, z) &= p(0, y, z) - \Delta p, & v(1, y, z) &= v(0, y, z), \\ p(x, 1, z) &= p(x, 0, z), & v(x, 1, z) &= v(x, 0, z), \\ p(x, y, 1) &= p(x, y, 0), & v(x, y, 1) &= v(x, y, 0). \end{aligned}$$

Periodic BC yields a symmetric and positive definite tensor.

Boundary conditions:

BC1: $p = 1$ at $(x, y, 0)$, $p = 0$ at $(x, y, 1)$, else no-flow (flow from left to right).

BC2: $p = 1$ at $(0, 0, 0)$, $p = 0$ at $(1, 1, 1)$, else no-flow (flow from corner to opposite corner).

Relative flow rate error	Stratified model		Unstratified model	
	BC1	BC2	BC1	BC2
Harm.–Arit.	1	1.14	0.081	0.155
Fixed BC	1	1.14	1	1.893
Periodic BC	1	1.14	0.986	1.867

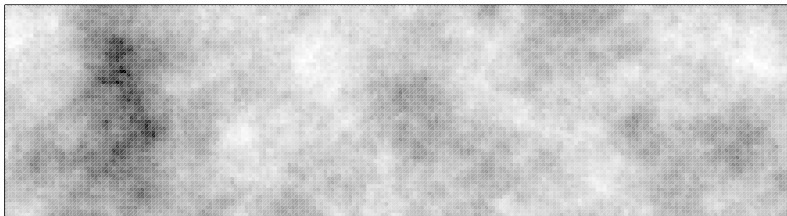
Upscaling

by design of a coarse simulation model has been, and still is, the default (and only) way that industry employs to fit the simulation model to the capabilities of commercial reservoir simulators.

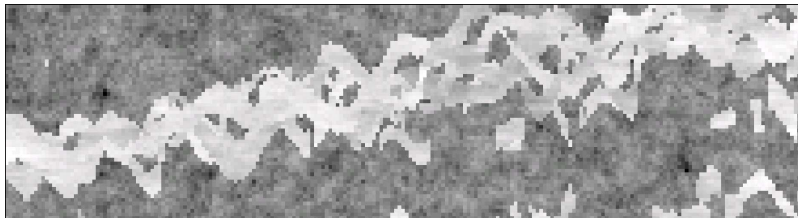
But ...

- Upscaling depends on flow regime.
- The favorite and most robust upscaling methods are designed for grids with shoe-box shaped grid blocks.
- Upscaling is inadequate for modeling flow in carbonate reservoirs, channelized reservoirs, or reservoirs where fine scale features that are not resolved by the coarse grid have dominant impact on large scale flow patterns.

Examples of heterogeneous structures



Logarithm of permeability in a shallow-marine Tarbert formation.



Logarithm of permeability in a fluvial Upper Ness formation.

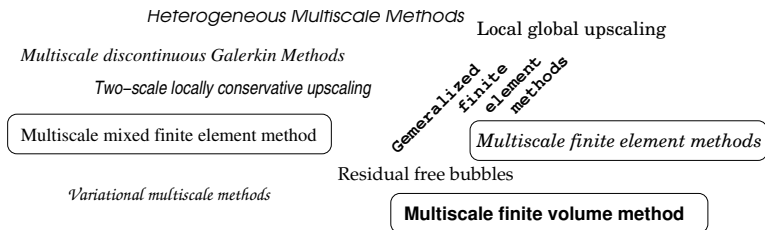
Exhale – inhale



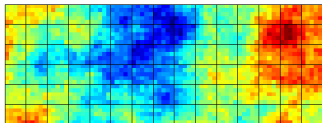
Multiscale methods coming up.

Multiscale methods:

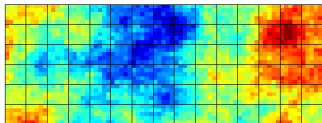
Numerical methods that attempt to model physical phenomena on coarse grids while honoring small-scale features that impact the coarse grid solution in an appropriate way.



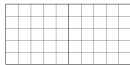
Standard upscaling:



Standard upscaling:

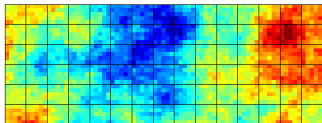


Coarse grid blocks:

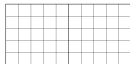


Flow based upscaling versus multiscale method

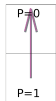
Standard upscaling:



Coarse grid blocks:

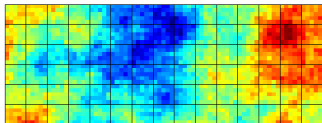


Flow problems:

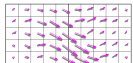


Flow based upscaling versus multiscale method

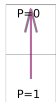
Standard upscaling:



Coarse grid blocks:

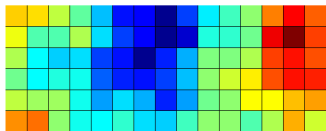


Flow problems:

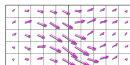


Flow based upscaling versus multiscale method

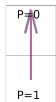
Standard upscaling:



Coarse grid blocks:

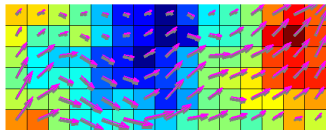


Flow problems:

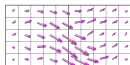


Flow based upscaling versus multiscale method

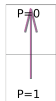
Standard upscaling:



Coarse grid blocks:

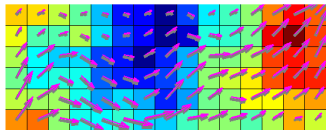


Flow problems:

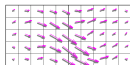


Flow based upscaling versus multiscale method

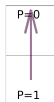
Standard upscaling:



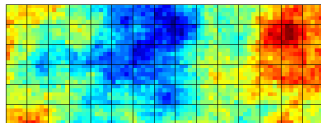
Coarse grid blocks:



Flow problems:

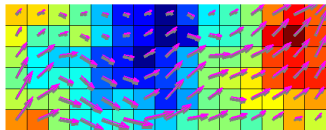


Multiscale method:

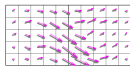


Flow based upscaling versus multiscale method

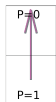
Standard upscaling:



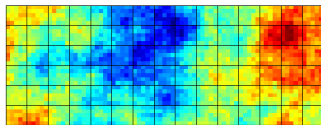
Coarse grid blocks:



Flow problems:



Multiscale method:



Coarse grid blocks:

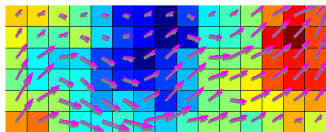


Flow problems:

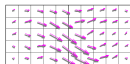


Flow based upscaling versus multiscale method

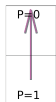
Standard upscaling:



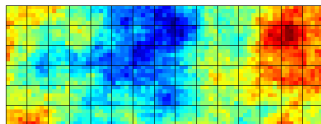
Coarse grid blocks:



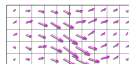
Flow problems:



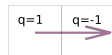
Multiscale method:



Coarse grid blocks:

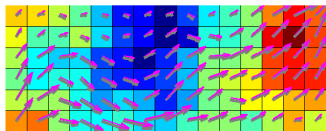


Flow problems:

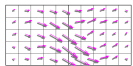


Flow based upscaling versus multiscale method

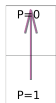
Standard upscaling:



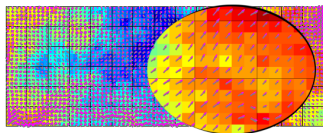
Coarse grid blocks:



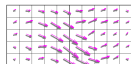
Flow problems:



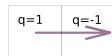
Multiscale method:



Coarse grid blocks:



Flow problems:



Model problem:

Consider the following elliptic problem:

$$\partial_x (k(x)\partial_x p) = f, \text{ in } \Omega = (0, 1), \quad p(0) = p(1) = 0,$$

where $f, k \in L^2(\Omega)$ and $0 < \alpha < k(x) < \beta$ for all $x \in \Omega$.

Variational formulation:

Find $p \in H_0^1(\Omega)$ such that

$$a(p, v) = (f, v) \quad \text{for all } v \in H_0^1(\Omega), \quad (1)$$

where (\cdot, \cdot) is the L^2 inner-product and

$$a(p, v) = \int_{\Omega} k(x)p'(x)v'(x) dx.$$

Multiscale finite-element method (MsFEM), 1D

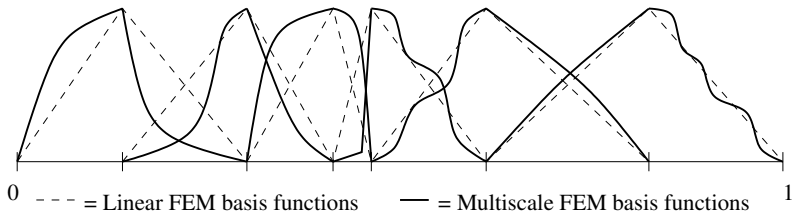
Let $\mathcal{N}_{\mathcal{K}} = \{0 = x_0 < x_1 < \dots < x_{n-1} < x_n = 1\}$ be a set of nodal points and define $K_i = (x_{i-1}, x_i)$.

For $i = 1, \dots, n - 1$ define a basis function $\phi^i \in H_0^1(\Omega)$ by

$$a(\phi^i, v) = 0 \quad \text{for all } v \in H_0^1(K_i \cup K_{i+1}), \quad \phi^i(x_j) = \delta_{ij},$$

where δ_{ij} is the Kronecker delta.

Basis functions:



MsMFEM:

Find the unique function p_0 in

$$\begin{aligned} V^{\text{ms}} &= \text{span}\{\phi_i\} \\ &= \{u \in H_0^1(\Omega) : a(u, v) = 0 \text{ for all } v \in H_0^1(\cup_i K_i)\} \end{aligned}$$

satisfying

$$a(p_0, v) = (f, v) \quad \text{for all } v \in V^{\text{ms}}.$$

Theorem

Assume p solves the variational formulation. Then $p = p_0 + \sum_{i=1}^n p_i$ where $p_i \in H_0^1(K_i)$ is defined by

$$a(p_i, v) = (f, v) \quad \text{for all } v \in H_0^1(K_i).$$

Galerkin projection property:

Assume p solves the variational formulation and $v \in V^{\text{ms}}$. Then

$$\begin{aligned} a(p - p_0, v) &= a(p, v) - a(p_0, v) \\ &= (f, v) - (f, v) = 0. \end{aligned}$$

Thus, p_0 is the orthogonal projection of p onto V^{ms} .

Since $H_0^1(\Omega) = V^{\text{ms}} \oplus H_0^1(\cup_i K_i)$ it follows that

$$p_0(x_i) = p(x_i) \quad \text{for all } i,$$

i.e., that p_0 is the interpolant of p in V^{ms} .

Proof II of super convergence property

Let p_I be the interpolant of p in V^{ms} . Then $p - p_I \in H_0^1(\cup_i K_i)$ and it follows from the mutual orthogonality of V^{ms} and $H_0^1(\cup_i K_i)$ with respect to $a(\cdot, \cdot)$ that

$$a(p - p_I, v) = 0 \quad \text{for all } v \in V^{\text{ms}}.$$

Hence,

$$a(p_I, v) = a(p, v) = (f, v) = a(p_0, v) \quad \text{for all } v \in V^{\text{ms}},$$

and we see that $a(p_I - p_0, v) = 0$ for all $v \in V^{\text{ms}}$. Thus, in particular, by choosing $v = p_I - p_0$ we obtain

$$a(p_I - p_0, p_I - p_0) = 0,$$

which implies $p_0 = p_I$.

Super convergence property:

Solution of the variational problem is decomposed into the MsFEM solution and solutions of independent local subgrid problems.

MsFEM in 1D = a Schur complement decomposition.

Super convergence property:

Solution of the variational problem is decomposed into the MsFEM solution and solutions of independent local subgrid problems.

MsFEM in 1D = a Schur complement decomposition.

Does the result extend to higher dimensions?

Super convergence property:

Solution of the variational problem is decomposed into the MsFEM solution and solutions of independent local subgrid problems.

MsFEM in 1D = a Schur complement decomposition.

Does the result extend to higher dimensions?

No, but the basic construction applies and helps us understand how subgrid features of the solution can be embodied into a coarse grid approximation space.

MsMFEM (for $-\nabla \cdot K(x)\nabla p = f$):

Find the unique function p_0 in

$$\begin{aligned} V^{\text{ms}} &= \text{span}\{\phi_{i,j}\} \\ &= \{u \in H_0^1(\Omega) : a(u, v) = 0 \text{ for all } v \in H_0^1(\cup_i K_i)\} \end{aligned}$$

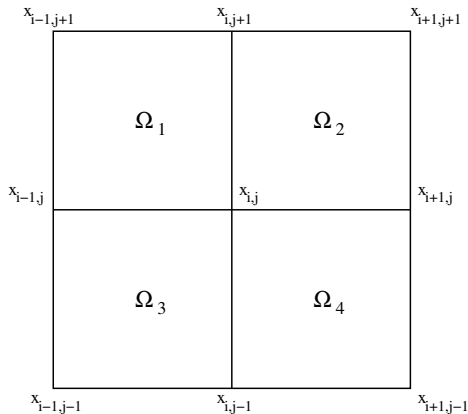
satisfying

$$a(p_0, v) = (f, v) \quad \text{for all } v \in V^{\text{ms}}.$$

Here (\cdot, \cdot) is the L^2 inner-product and

$$a(p, v) = \int_{\Omega} \nabla p \cdot K(x)\nabla v \, dx.$$

MsFEM basis functions in 2D

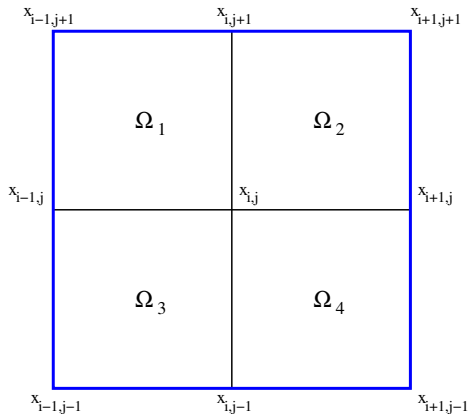


- $p \in V^{\text{ms}}$ implies that

$$\nabla \cdot K \nabla \phi_{i,j} = 0 \text{ in all } \Omega_m.$$

Note: If $p \in V^{\text{ms}}$ then $p_0 = p$ by projection property.

MsFEM basis functions in 2D



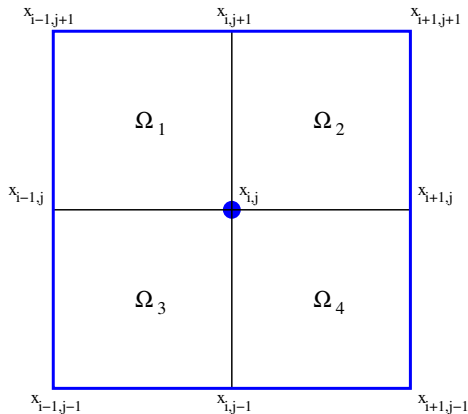
- $p \in V^{\text{ms}}$ implies that

$$\nabla \cdot K \nabla \phi_{i,j} = 0 \text{ in all } \Omega_m.$$

- $\phi_{i,j} = 0$ on edges not emanating from $x_{i,j}$.

Note: If $p \in V^{\text{ms}}$ then $p_0 = p$ by projection property.

MsFEM basis functions in 2D



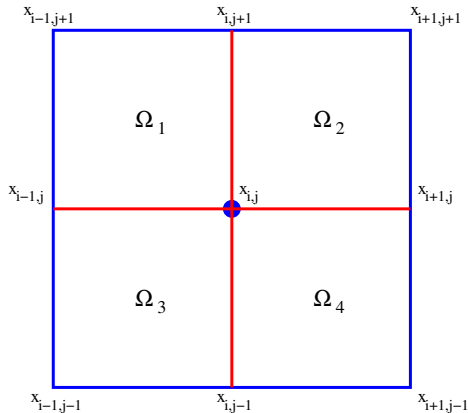
- $p \in V^{\text{ms}}$ implies that

$$\nabla \cdot K \nabla \phi_{i,j} = 0 \text{ in all } \Omega_m.$$

- $\phi_{i,j} = 0$ on edges not emanating from $x_{i,j}$.
- $\phi_{i,j}(x_{m,n}) = \delta_{i,m} \delta_{j,n}$.

Note: If $p \in V^{\text{ms}}$ then $p_0 = p$ by projection property.

MsFEM basis functions in 2D



- $p \in V^{\text{ms}}$ implies that

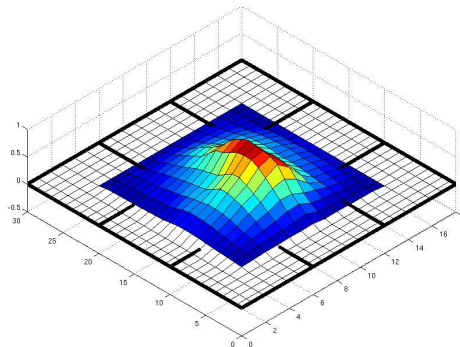
$$\nabla \cdot K \nabla \phi_{i,j} = 0 \text{ in all } \Omega_m.$$

- $\phi_{i,j} = 0$ on edges not emanating from $x_{i,j}$.
- $\phi_{i,j}(x_{m,n}) = \delta_{i,m} \delta_{j,n}$.
- **Boundary conditions on edges emanating from $x_{i,j}$?**

Note: If $p \in V^{\text{ms}}$ then $p_0 = p$ by projection property.

Multiscale finite volume method (MsFVM)

is a control-volume finite-element version of the MsFEM. A CVFE method seeks solutions in a finite-element space (on a dual-grid), but rather than formulating the problem in a variational framework, it employs instead a finite-volume formulation (on a primal grid).



MsFEM basis function on a dual grid connecting cell centers of the primal grid.

Boundary conditions on “interior edges” derived by solving reduced dimensional pressure equation.

Step 1: Compute basis functions ϕ_i (ϕ_i denotes the basis function associated with the center of Ω_i).

Step 2: Find $p = \sum_i p_i \phi_i$ such that

$$-\int_{\partial\Omega_j} K \nabla p \cdot n \, ds = \int_{\Omega_j} f \, dx.$$

Step 3: Downscale to obtain a mass conservative velocity field

$$\begin{aligned} v &= -K \nabla u && \text{in all } \Omega_j, \\ \nabla \cdot v &= f && \text{in all } \Omega_j, \\ v &= -K \nabla p && \text{on all } \partial\Omega_j. \end{aligned}$$

Complexity and robustness issues for MsFVM

- Inaccurate for high-aspect ratios or cases with large anisotropy.
- Difficult to implement for complex grids, e.g., it is difficult to define a dual grid if primal grid honors geological features.
- No escaping downscaling for multi-phase flows; computational cost comparable to a domain decomposition sweep.
- Accuracy depends highly on proper boundary conditions.

Multiscale mixed finite element method (MsMFEM)

Pressure eq.: $v = -\lambda(\nabla p + \omega g \nabla z)$ and $\nabla \cdot v = q$.

Mixed formulation (no-flow boundary conditions):

Find $p \in U \subset L^2(\Omega)$ and $v \in V \subset H_0^{\text{div}}(\Omega)$ such that

$$\int_{\Omega} v \cdot \lambda^{-1} u \, dx - \int_{\Omega} p \nabla \cdot u \, dx = - \int_{\Omega} \omega g \nabla z \cdot u \, dx,$$
$$\int_{\Omega} l \nabla \cdot v \, dx = \int_{\Omega} ql \, dx,$$

for all $u \in V$ and $l \in U$.

Multiscale mixed finite element method (MsMFEM):

Mixed finite element method for which V is designed to embody the impact of fine scale structures.

Multiscale mixed finite element method

Basis functions

Associate a basis function χ_m for **pressure** with each grid block K :

$$U = \text{span}\{\chi_m : K_m \in \mathcal{K}\} \quad \text{where} \quad \chi_m = \begin{cases} 1 & \text{if } x \in K_m, \\ 0 & \text{else,} \end{cases}$$

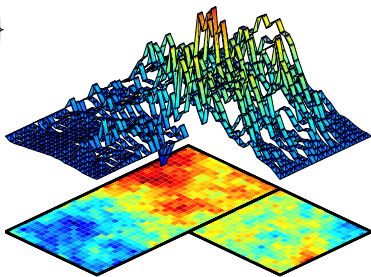
and a **velocity** basis function ψ_{ij} with each interface $\partial K_i \cap \partial K_j$:

$$V = \text{span}\{\psi_{ij} = -k\nabla\phi_{ij}\}$$

$$\psi_{ij} \cdot n = 0 \quad \text{on } \partial(K_i \cup K_j)$$

$$\nabla \cdot \psi_{ij} = \begin{cases} w_i(x) & \text{in } K_i, \\ -w_j(x) & \text{in } K_j. \end{cases}$$

where w_i is a weight function with $\int_{K_i} w_i(x) dx = 1$.

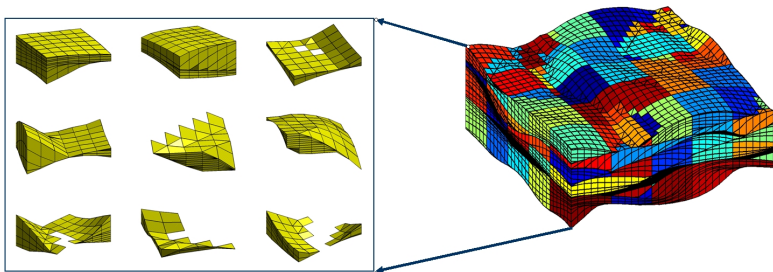


Multiscale mixed finite element method

Coarse grid

Each coarse grid block is a connected set of cells from geomodel.

Example: Coarse grid obtained with uniform coarsening in index space.

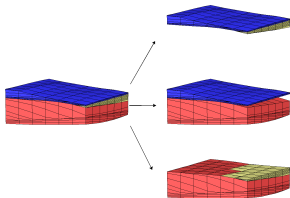


Grid adaptivity at well locations:

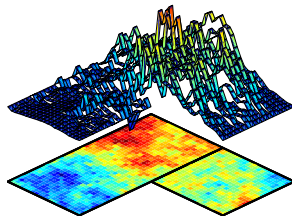
One block assigned to each cell in geomodel with well perforation.

At initial time

Detect all adjacent blocks



Compute ψ for each domain



For each time-step:

- Assemble and solve coarse grid system.
- Recover fine grid velocity: $v = \sum_{ij} v_{ij} \psi_{ij}$.
- Solve mass balance equations.

Multiscale mixed finite element method

Layer 36 from SPE10 model 2 (Christie and Blunt, 2001).

Example: Layer 36 from SPE10 (Christie and Blunt, 2001).

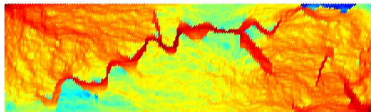
Pressure field computed with mimetic FDM



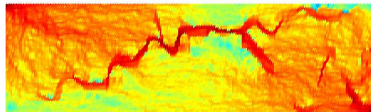
Pressure field computed with 4M



Velocity field computed with mimetic FDM



Velocity field computed with 4M



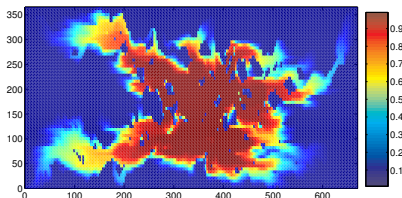
Primary features

- Coarse pressure solution, subgrid resolution at well locations.
- Coarse velocity solution with subgrid resolution everywhere.

Numerical example

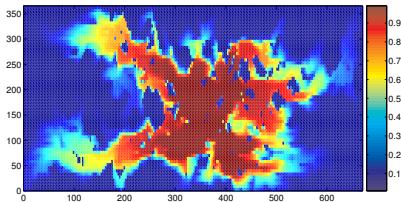
Layer 85 from SPE10 model 2 (Christie and Blunt, 2001).

Pressure computed on fine grid

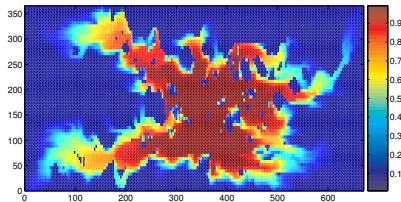


- Water injected at center of an oil-filled reservoir. Producer at each corner.
- Geomodel: 60×220 grid.
- Figures: water fraction when volume injected = 30% of total flow volume.

MsFVM: coarse grid = 10×44



MsMFEM: coarse grid = 10×44



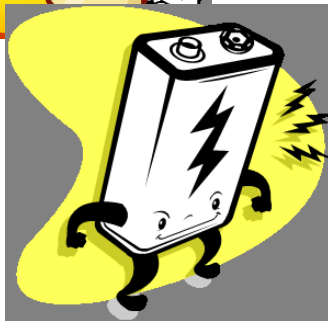
11.20



11.25



11.30



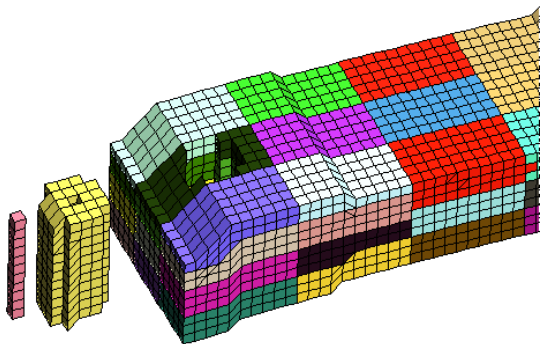
- Coarse grid generation
- Choice of weighting function in definition of basis functions.
- Incorporation of global information in basis functions.
- Choice of numerical method for computation of basis functions
- Assembly of linear system

MsMFEM (unique) grid flexibility:

Given a method applicable to solving the local flow problems on the subgrid, the MsMFEM can be formulated on any coarse grid where each grid block consists of a connected collection fine-grid cells.

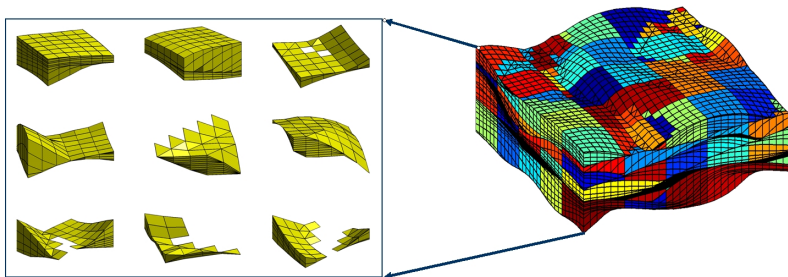
MsMFEM (unique) grid flexibility:

Given a method applicable to solving the local flow problems on the subgrid, the MsMFEM can be formulated on any coarse grid where each grid block consists of a connected collection fine-grid cells.



MsMFEM (unique) grid flexibility:

Given a method applicable to solving the local flow problems on the subgrid, the MsMFEM can be formulated on any coarse grid where each grid block consists of a connected collection fine-grid cells.



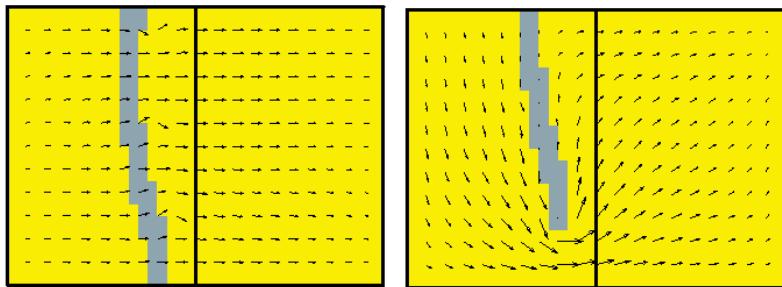
MsMFEM (unique) grid flexibility:

Given a method applicable to solving the local flow problems on the subgrid, the MsMFEM can be formulated on any coarse grid where each grid block consists of a connected collection fine-grid cells.

The process of generating a coarse simulation grid from a complex geological model can be greatly simplified, especially when the fine grid is fully unstructured or has geometrical complications.

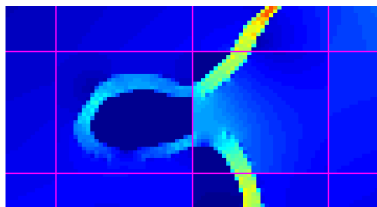
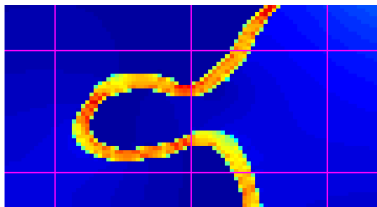
Limitations:

- Limited ability to model flow around large scale flow barriers



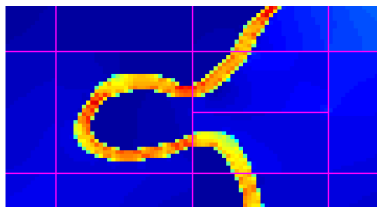
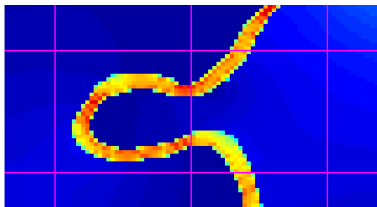
Limitations:

- Limited ability to model flow around large scale flow barriers
- Limited ability to model bi-directional flow across interfaces.



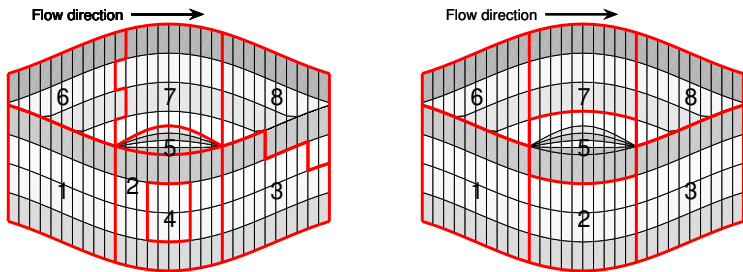
Limitations:

- Limited ability to model flow around large scale flow barriers
- Limited ability to model bi-directional flow across interfaces.



Coarse grid generation

Guidelines

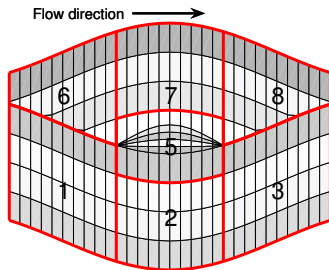
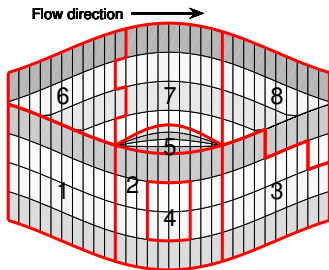


Guidelines:

- 1: The coarse grid should minimize the occurrence of bi-directional flow across interfaces. Grid structures that increase the likelihood for bidirectional flow are:
 - Coarse-grid faces with (highly) irregular shapes.
 - Blocks that have only one neighbor.
 - Blocks with no faces transverse to the major flow directions.

Coarse grid generation

Guidelines

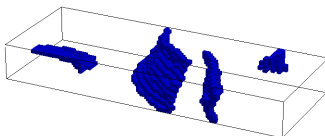
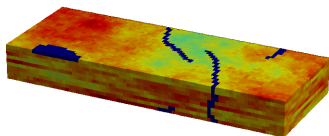


Guidelines:

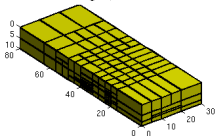
- 2: Blocks should follow geological layers when possible.
 - Avoids disrupting flow patterns.

Guidelines:

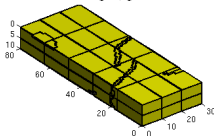
3: Blocks in the coarse-grid should adapt to flow barriers.



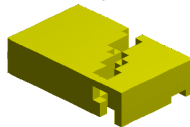
Non-uniform grid, hexahedral cells



Non-uniform grid, general cells

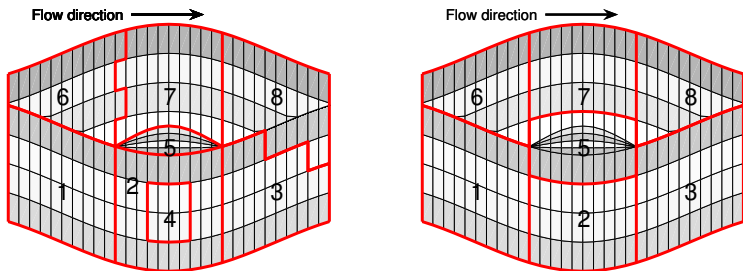


General grid-cell



Coarse grid generation

Guidelines



Note: It may be difficult to obtain an 'optimal' coarse grid, since guidelines may be in conflict with each other, but this is not necessary since the MsMFEM is quite robust. Efforts to improve the coarse grid is generally only needed in *extreme* cases.

Choice of numerical method

Any conservative method may be used to compute basis functions, but it is convenient to use a mixed FEM or a mimetic FDM.

Assembly of linear system

Let the linear system

$$\begin{bmatrix} \mathbf{B} & -\mathbf{C}^T \\ \mathbf{C} & \mathbf{0} \end{bmatrix} \begin{bmatrix} \mathbf{v} \\ \mathbf{p} \end{bmatrix} = \begin{bmatrix} \mathbf{g} \\ \mathbf{q} \end{bmatrix}$$

stem from a mixed FEM or mimetic FDM discretization on the entire subgrid. Use the same method to compute basis functions so that each multiscale basis function Ψ_{ij} is a linear combination of the mixed FEM or mimetic FDM velocity basis functions ψ_{kl} .

Assembly of linear system, cont.

Let \mathbf{r}_{ij} be the vector holding the coefficients r_{kl}^{ij} in the expansion

$$\Psi_{ij} = \sum_{\gamma_{kl}} r_{kl}^{ij} \psi_{kl},$$

and let \mathbf{R} be the corresponding matrix with columns \mathbf{r}_{ij} .

Then the linear system for the MsMFEM takes the following form:

$$\begin{bmatrix} \mathbf{R}^t \mathbf{B} \mathbf{R}^t & -\mathbf{C}_c^T \\ \mathbf{C}_c & \mathbf{0} \end{bmatrix} \begin{bmatrix} \mathbf{v} \\ \mathbf{p}_c \end{bmatrix} = \begin{bmatrix} \mathbf{R}^t \mathbf{g} \\ \mathbf{q}_c \end{bmatrix},$$

where $\mathbf{q}_c = [\int_{K_i} q \, dx]$, and $\mathbf{C}_c = [c_{m,ij}]$ where $c_{m,ij} = \delta_{im} - \delta_{jm}$.

The coarse system is obtained from the fine grid system!

Role of weight functions

Let $(w_m, 1)_m = 1$ and let v_m^i be coarse-scale coefficients.

$$v = \sum v_{ij} \psi_{ij} \quad \Rightarrow \quad (\nabla \cdot v)|_{K_i} = w_i \sum_j v_{ij} = w_i \int_{K_i} \nabla \cdot v \, dx.$$

→ w_m gives distribution of $\nabla \cdot v$ among cells in geomodel.

Incompressible flow: $\nabla \cdot v = q.$

Black-oil model: $\nabla \cdot v = q - c_t \frac{\partial p}{\partial t} - \sum_j c_j v_j \cdot \nabla p.$

Incompressible flow

$$(\nabla \cdot v)|_{K_i} = w_i \sum_j v_{ij}$$

where

$$\sum_j v_{ij} = \begin{cases} 0 & \text{if } \int_{K_i} q \, dx = 0, \\ \int_{K_i} q \, dx & \text{otherwise.} \end{cases}$$

Thus,

$$\int_{K_i} q \, dx = 0 \quad \Rightarrow \quad \nabla \cdot v = 0 \text{ for all } w_i > 0.$$

$$\int_{K_i} q \, dx \neq 0 \quad \Rightarrow \quad \nabla \cdot v = q \text{ if } w_i = \frac{q}{\int_{K_i} q \, dx}.$$

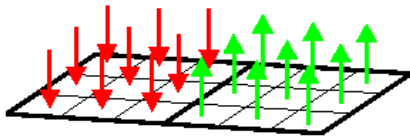
Choice of weight functions in blocks with $\int_{K_i} q \, dx = 0$.

Incompressible flow

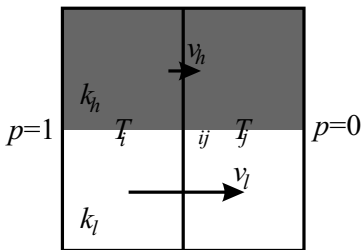
Uniform source:

$$w_i = |K_i|^{-1}.$$

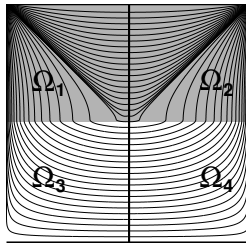
(Chen and Hou, 2003).



Example: layered media, flow from left to right.



Top half: low permeability
Bottom half: high permeability



Streamlines from MsMFEM
basis function.

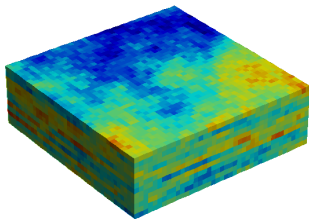
Choice of weight functions in blocks with $\int_{K_i} q dx = 0$.

Incompressible flow

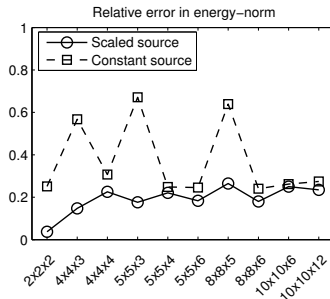
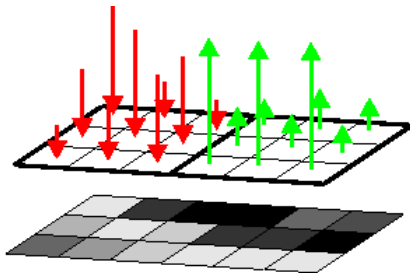
Scaled source:

$$w_i = \frac{K(x)}{\int_{K_i} K(x) dx}.$$

(Aarnes, Krogstad and Lie, SIAM MMS 2006).



Sample from model 2, SPE10



Compressible flow

$$(\nabla \cdot v)|_{K_i} = w_i \sum_j v_{ij}$$

where

$$\sum_j v_{ij} = \int_{K_i} q - c_t \frac{\partial p}{\partial t} - \sum_j c_j v_j \cdot \nabla p \, dx.$$

- $w_i = \frac{q}{\int_{K_i} q \, dx}$ concentrates compressibility effects where $q \neq 0$.
- $w_i \propto K$ gives velocity fields where $\text{div}(v)$ is underestimated in low-perm. regions and overestimated in high-perm. regions.

Remedy:

- Separate sources and compressibility effects by assigning a separate coarse grid block to each cell with a source.
- Let $w_i = \frac{\phi}{\int_{K_i} \phi \, dx}$ where ϕ is the porosity.

Invoking global information

An alternative to grid refinement (e.g., near barriers) is to use global information to improve the MsMFEM solution.

Mixed formulation: Find $p \in L^2(\Omega)$ and $v \in H_0^{\text{div}}(\Omega)$ such that

$$\begin{aligned} \int_{\Omega} v \cdot \lambda^{-1} u \, dx - \int_{\Omega} p \nabla \cdot u \, dx &= - \int_{\Omega} \omega g \nabla z \cdot u \, dx \quad \forall u \in H_0^{\text{div}}(\Omega), \\ \int_{\Omega} l \nabla \cdot v \, dx &= \int_{\Omega} q l \, dx \quad \forall l \in L^2(\Omega). \end{aligned}$$

MsMFEM: Find $p_h \in U$ and $v_h \in V^{\text{ms}}$ such that

$$\begin{aligned} \int_{\Omega} v_h \cdot \lambda^{-1} u \, dx - \int_{\Omega} p_h \nabla \cdot u \, dx &= - \int_{\Omega} \omega g \nabla z \cdot u \, dx \quad \forall u \in V^{\text{ms}}, \\ \int_{\Omega} l \nabla \cdot v_h \, dx &= \int_{\Omega} q l \, dx \quad \forall l \in U. \end{aligned}$$

Invoking global information

Since $V^{\text{ms}} \subset H_0^{\text{div}}(\Omega)$ and $U \subset L^2(\Omega)$ we have

$$\int_{\Omega} v \cdot \lambda^{-1} u \, dx - \int_{\Omega} p \nabla \cdot u \, dx = - \int_{\Omega} \omega g \nabla z \cdot u \, dx \quad \forall u \in V^{\text{ms}},$$
$$\int_{\Omega} l \nabla \cdot v \, dx = \int_{\Omega} ql \, dx \quad \forall l \in U.$$

Assume that $v \in V^{\text{ms}}$, define

$$p_h = \sum p_i \chi_i \quad \text{where} \quad p_i = \int_{K_i} p w_i \, dx.$$

and note that

$$\begin{aligned} \int_{\Omega} p \nabla \cdot u \, dx &= \sum_{ij} (\int_{K_i} p w_i \, dx - \int_{K_j} p w_j \, dx) \\ &= \sum_{ij} (p_i - p_j) = \int_{\Omega} p_h \nabla \cdot u \, dx. \end{aligned}$$

Hence: v and p_h is the MsMFEM solution.

Key observation:

If $v \in V^{\text{ms}}$ then the MsMFEM replicates v (i.e., $v_h = v$) regardless of heterogeneity (barriers, channels, etc.) and grid.

The pressure p_h is an exact w -weighted average in each grid block

$$p_h|_{K_i} = \int_{K_i} p w_i dx.$$

Question:

Is it possible to define basis functions so that $v \in V^{\text{ms}}$?

Yes, $v \in V^{\text{ms}}$ if

$$\Psi_{ij} \cdot n_{ij} = \frac{v \cdot n_{ij}}{\int_{\partial K_i \cap \partial K_j} v \cdot n_{ij} ds}.$$

Assume that we have computed v , e.g., on a fine grid.

Global basis functions:

$$\begin{aligned}\psi_{ij} \cdot n &= 0 \text{ on } \partial(K_i \cup K_j) \\ \nabla \cdot \psi_{ij} &= \begin{cases} w_i(x) & \text{in } K_i, \\ -w_j(x) & \text{in } K_j. \end{cases} \\ \Psi_{ij} \cdot n_{ij} &= \frac{v \cdot n_{ij}}{\int_{\partial K_i \cap \partial K_j} v \cdot n_{ij} ds}.\end{aligned}$$

Why?

Because in multiphase flow simulation the pressure equation needs to be resolved many times (due to changes in the flow mobility), but the basis functions need only be computed once.



I want you!

Vacant position:

Postdoctoral researcher
in reservoir modeling
and simulation: see
www.sintef.no.

Key technologies:

- Multiscale methods
- Streamline methods
- Grid generation
- Parallel computing
- GPU computing

Closing date: June 11.

Send applications to:

Jorg.Aarnes@sintef.no